Bioconjugate Chemistry

Article

pubs.acs.org/bc

Heavy Atom Containing Fluorescent Ribonucleoside Analog Probe for the Fluorescence Detection of RNA-Ligand Binding

Maroti G. Pawar, Ashok Nuthanakanti, and Seergazhi G. Srivatsan*

Department of Chemistry, Indian Institute of Science Education and Research, Dr. Homi Bhabha Road, Pashan, Pune 411008, India

Supporting Information

ABSTRACT: Although numerous biophysical tools have provided effective systems to study nucleic acids, our current knowledge on how RNA structure complements its function is limited. Therefore, development of robust tools to study the structure–function relationship of RNA is highly desired. Toward this endeavor, we have developed a new ribonucleoside analog, based on a (selenophen-2-yl)pyrimidine core, which could serve as a fluorescence probe to study the function of RNA in real time and as an anomalous scattering label (selenium atom) for the phase determination in X-ray crystallography. The fluorescent selenophene-modified uridine analog is minimally perturbing and exhibits probe-like properties such as sensitivity to microenvironment and conformation changes. Utilizing these properties and amicability of the corresponding ribonucleotide analog to enzymatic incorporation, we have synthesized a fluorescent bacterial ribosomal decoding site (A-site) RNA construct and have developed a fluorescence binding assay to effectively monitor the binding of aminoglycoside antibiotics to the A-site. Our results demonstrate that this simple approach of building a dual probe could provide new avenues to study the structure–function relationship of not only nucleic acids, but also other biomacromolecules.

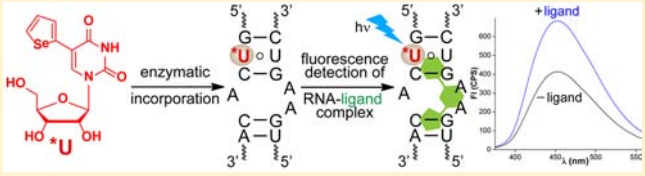

INTRODUCTION

Ribonucleic acid participates in a multitude of essential cellular processes including catalysis, and maintenance and regulation of genetic information by interacting with proteins, nucleic acids, and small molecule metabolites. Despite limited chemical diversity as compared to proteins, RNA expands its functional repertoire by utilizing its intrinsic conformational dynamics and by adopting diverse secondary and tertiary structures.[1−4] Several techniques such as fluorescence, electrophoresis, nuclear magnetic resonance, electron paramagnetic resonance, to name a few, have been very useful in advancing our understanding of the structure, dynamics, and recognition properties of nucleic acids.[5−9] In parallel, high-resolution X-ray structures of a significant number of functional RNA motifs have provided better insights into the relationship between RNA structure and function at the molecular level.[10,11]

Needless to say, several of the biophysical tools require appropriately labeled nucleic acid reporters.[12−14] In this context, oligonucleotides (ONs) labeled with fluorescent nucleoside analogs that signal changes in their local environment via changes in their fluorescence properties—quantum yield, emission maximum, lifetime, and anisotropy—have been very useful in devising several nucleic acid-based bioanalytical and discovery assays.[15−26] Similarly, 3-D structure determination of nucleic acids by X-ray crystallography has greatly relied on heavy atom derivatization of nucleic acids for phase determination. Conventionally, the anomalous scattering from a bromine or iodine atom of brominated or iodinated nucleic acids is used in determining the structures by single-wavelength anomalous dispersion (SAD) phasing or by multiwavelength anomalous dispersion (MAD) phasing techniques.[27,28] Subsequently, the superior anomalous scattering property of selenium atom that has been extensively exploited in protein X-ray crystallography has also been extended to nucleic acid X-ray crystallography.[29,30] Huang, Egli, and co-workers for the first time used Se-MAD phasing technique to report the X-ray structure of selenium-modified DNA and RNA oligonucleotides obtained via phosphoroselenoate backbone modification and 2′-methylselenouridine modification, respectively.[31−34] Later, methods have been developed to introduce selenium atom into oligonucleotides by using native nucleosides with 2′-methylseleno group or by replacing the base oxygen atoms with selenium.[35−37] These heavy atom derivatization methodologies have been successfully utilized in the X-ray structure determination of nucleic acids, and nucleic acid–protein and nucleic acid–small molecule complexes.[31−34,38−42]

The amount of information and fundamental knowledge we have gained on the structure and function of certain nucleic acid motifs through these experiments is arguably undeniable. Nevertheless, the rate at which new functional RNAs are being discovered, and since the current knowledge on the structure–function relationship of RNA is limited, it is essential to develop robust tools to understand how RNA structure complements its function. Toward this endeavor, it is highly desirable to develop a label compatible with two complementing biophysical techniques, one that would provide information on the

Received: April 17, 2013
Revised: June 12, 2013
Published: July 10, 2013

dynamics and recognition properties in real time and the other on the 3D structure of nucleic acids. For example, incorporating a conformation-sensitive fluorescent nucleoside analog probe, containing an anomalous scattering atom (e.g., selenium), into nucleic acids would allow the analysis of structure−function relationship by both fluorescence and X-ray crystallography techniques. Literature reports indicate that minimally perturbing fluorescent nucleoside analog probes can be assembled by attaching or fusing heterocyclic rings onto nucleobases.[15,43−48] In particular, Tor and co-workers have developed fluorescent nucleoside analogs by conjugating furan at the 5-position of uracil, and have utilized them in devising assays to detect the presence of DNA abasic sites and the binding of aminoglycoside antibiotics to RNA.[49,50] Drawing inspiration from these reports, we hypothesized that the conjugation of a selenophene moiety at the 5-position of uracil would generate a minimally perturbing emissive nucleobase analog, which could serve as a fluorescence probe as well as an anomalous scattering label for the phase determination in X-ray crystallography. Here, we describe the synthesis and photophysical characterization of a new emissive uridine analog **2**, based on a (selenophen-2-yl)pyrimidine core. Notably, the selenophene-conjugated uridine analog displays emission in the visible region and very good fluorescence solvatochromism. Furthermore, as a proof of responsiveness of the nucleoside to RNA conformational changes, we have enzymatically labeled a therapeutically important RNA motif, ribosomal decoding site (A-site), with the emissive nucleoside **2**, and have developed a fluorescence binding assay to effectively monitor the binding of aminoglycoside antibiotics to the bacterial A-site.

EXPERIMENTAL SECTION

Materials. 5-Iodouridine, selenophene, tributyltin chloride, and *bis*(triphenylphosphine)-palladium(II) chloride were obtained from Sigma-Aldrich. $POCl_3$ was purchased from Acros Organics, and was distilled before use. Paromomycin and neomycin were purchased from Sigma-Aldrich. Synthetic DNA ONs were either purchased from Integrated DNA Technologies, Inc., or from Sigma-Aldrich. ONs were purified by polyacrylamide gel electrophoresis (PAGE) under denaturing conditions, and desalted on Sep-Pak Classic C18 cartridges (Waters Corporation). Custom synthesized oligoribonucleotides purchased from Dharmacon RNAi Technologies were deprotected according to the supplier's instructions, PAGE-purified, and desalted on Sep-Pak Classic C18 cartridges. T7 RNA polymerase, ribonuclease inhibitor (RiboLock), RNase A, RNase T1, and NTPs were obtained from Fermentas Life Science. Calf intestinal alkaline phosphatase was purchased from Invitrogen. Snake venom phosphodiesterase I was purchased from Sigma-Aldrich. Radiolabeled α-^{32}P ATP (2000 Ci/mmol) was obtained from the Board of Radiation and Isotope Technology, Government of India. Chemicals for preparing buffer solutions were purchased from Sigma-Aldrich (BioUltra grade). Autoclaved water was used in all biochemical reactions and fluorescence measurements.

Instrumentation. NMR spectra were recorded on a 400 MHz Jeol ECS-400. All mass measurements were recorded on an Applied Biosystems 4800 Plus MALDI TOF/TOF analyzer and Water Synapt G2 High Definition mass spectrometer. Absorption spectra were recorded on a PerkinElmer, Lambda 45 UV−vis spectrophotometer. UV-thermal melting analysis was performed on a Cary 300Bio UV−vis spectrophotometer. Steady state fluorescence experiments were performed on a Fluoromax-4 spectrophotometer (Horiba Jobin Yvon) and time-resolved fluorescence experiments were carried on a TCSPC instrument (Horiba Jobin Yvon, Fluorolog-3, and Horiba Jobin Yvon, IBH, USA) in a micro fluorescence cuvette (Hellma, path length 1.0 cm). Reversed-phase (RP) flash chromatography (C18 Redi*SepRf* column) purifications were carried out using Teledyne ISCO, Combi Flash Rf. Agilent technologies HPLC (1260 infinity) was used for RP-HPLC analysis. Phosphorimages were recorded on a Typhoon Trio+, GE-Healthcare.

Selenophene-Conjugated Uridine 2. To a suspension of 5-iodouridine (0.250 g, 0.68 mmol, 1.00 equiv) and *bis*(triphenylphosphine)-palladium(II) chloride (0.024 g, 0.034 mmol, 0.05 equiv) in degassed anhydrous dioxane (7.5 mL) was added 2-(tributylstannyl)selenophene[51] (0.425 g, 1.01 mmol, 1.5 equiv). The reaction mixture was heated at 90 °C for 2 h and was cooled to RT. The reaction mixture was then filtered through a Celite pad and washed with hot dioxane (3 × 10 mL). The filtrate was concentrated and precipitated with petroleum ether. The precipitated crude product was purified by flash chromatography using a C18 RP column (C18 Redi*SepRf* 43 g column, 10−55% acetonitrile in water for 35 min) to afford the product as a white solid (0.115 g, 46%). TLC ($CHCl_3$:MeOH = 80:20) R_f = 0.63; ^{1}H NMR (400 MHz, d_6-DMSO): δ = 11.81 (s, 1H), 8.80 (s, 1H), 8.08 (d, J = 5.6 Hz, 1H), 7.60 (d, J = 3.6 Hz, 1H), 7.28 (dd, J = 5.6 Hz, J = 4.0 Hz, 1H), 5.84 (d, J = 3.6 Hz, 1H), 5.51−5.49 (m, 2H), 5.11 (d, J = 5.2 Hz, 1H), 4.13 (dd, J = 9.2 Hz, J = 4.8 Hz, 1H), 4.07 (dd, J = 10.4 Hz, J = 5.2 Hz, 1H), 3.93−3.92 (m, 1H), 3.81−3.76 (m, 1H), 3.68−3.63 (m, 1H) ppm; ^{13}C NMR (100 MHz, d_6-DMSO): δ = 161.8, 149.4, 137.6, 134.5, 131.7, 128.6, 122.8, 109.9, 88.9, 84.6, 74.4, 69.2, 60.0 ppm; HRMS: m/z Calcd. for $C_{13}H_{14}N_2O_6SeNa$ $[M+Na]^+$: 396.9915; found: 396.9873; λ_{max} (H_2O) = 273 and 325 nm, ε_{273} = 9990 M^{-1} cm^{-1}, ε_{325} = 9221 M^{-1} cm^{-1}, ε_{260} = 8576 M^{-1} cm^{-1}.

Selenophene-Conjugated UTP 3. To an ice-cold solution of ribonucleoside **2** (0.070 g, 0.19 mmol, 1 equiv) in trimethyl phosphate (1 mL) was added freshly distilled $POCl_3$ (45 μL, 0.48 mmol, 2.5 equiv). The solution was stirred for 29 h at ∼4 °C. TLC revealed only partial conversion of the ribonucleoside to the monophosphorylated nucleoside intermediate. A solution of *bis*-tributylammonium pyrophosphate[52] (0.5 M in DMF, 2 mL, 5.3 equiv) and tributylamine (0.5 mL, 2.12 mmol, 11.3 equiv) was rapidly added under ice-cold conditions. The reaction was quenched after 30 min with 1 M triethylammonium bicarbonate buffer (TEAB, pH 7.5, 15 mL) and was extracted with ethyl acetate (20 mL). The aqueous layer was evaporated and the residue was purified first on DEAE sephadex-A25 anion exchange column (10 mM to 1 M TEAB buffer, pH 7.5) followed by RP flash column chromatography (C18 Redi*SepRf*, 0−40% acetonitrile in 50 mM triethylammonium acetate buffer, pH 7.2, 40 min). Appropriate fractions were lyophilized to afford the desired triphosphate product **3** as a tetratriethylammonium salt (34 mg, 18%). ^{1}H NMR (400 MHz, D_2O): δ = 8.17 (s, 1H), 8.10 (d, J = 5.6, 1H), 7.71 (d, J = 3.2, 1H), 7.36 (dd, J = 5.2 Hz, J = 4.0 Hz, 1H), 5.98 (d, J = 4.8, 1H), 4.45−4.44 (m, 2H), 4.28−4.25 (m, 3H) ppm; ^{13}C NMR (100 MHz, D_2O): δ = 163.2, 150.7, 135.9, 134.5, 132.3, 129.7, 125.7, 112.0, 88.6, 83.7, 73.9, 69.9, 65.4 ppm; ^{31}P NMR (162 MHz, D_2O): δ = −6.94 (d, J = 15.2 Hz), −11.63 (d, J = 16.0 Hz), −22.54 (t, J = 15.6 Hz) ppm; HRMS: m/z Calcd. for $C_{13}H_{17}N_2O_{15}P_3Se$ [M]: 613.9007, found: 612.8951 $[M-H]^-$.

Photophysical Characterization of Ribonucleoside 2 in Various Solvents. *Absorption Spectroscopy.* Absorption spectra of selenophene-modified ribonucleoside **2** (50 μM) was recorded in water, methanol, and dioxane. All solutions contained 5% DMSO. All experiments were performed in triplicate in a micro cuvette (Hellma, path length 1.0 cm) on a PerkinElmer, Lambda 45 UV−vis spectrophotometer.

Steady-State Fluorescence. Steady-state fluorescence of ribonucleoside **2** (5 μM) was recorded by exciting at respective lowest energy absorption maximum with an excitation slit width of 6 nm and emission slit width of 9 nm. All solutions contained 0.5% DMSO. Fluorescence experiments were performed in triplicate in a micro fluorescence cell (Hellma, path length 1.0 cm).

Time-Resolved Fluorescence Measurements. Excited-state lifetimes of **2** (250 μM) were determined using TCSPC instrument. Fluorescently modified ribonucleoside **2** was excited using 375 nm diode laser source (IBH, UK, NanoLED-375L) with a band-pass of 10 nm and fluorescence signal at respective emission maximum was collected. Lifetime measurements were performed in duplicate and decay profiles were analyzed using IBH DAS6 analysis software. Fluorescence intensity decay profiles in all solvents were found to be biexponential with $\chi 2$ (goodness of fit) values very close to unity.

Enzymatic Incorporation of Ribonucleoside Triphosphate 3. *Transcription Reactions in the Presence of α-^{32}P ATP.* Promoter-template duplexes were assembled by heating a 1:1 concentration (final 5 μM) of DNA ON templates (**T1**−**T5**) and an 18-mer T7 RNA polymerase consensus promoter DNA ON sequence in TE buffer (10 mM Tris-HCl, 1 mM EDTA, 100 mM NaCl, pH 7.8) at 90 °C for 3 min and cooling the solution slowly to RT. The duplexes were then placed on crushed ice for 30 min and stored at −40 °C. Transcription reactions were performed in 40 mM Tris-HCl buffer (pH 7.9) containing 250 nM promoter-template duplexes, 10 mM $MgCl_2$, 10 mM NaCl, 10 mM dithiothreitol (DTT), 2 mM spermidine, 1 U/μL RNase inhibitor (RiboLock), 1 mM GTP, 1 mM CTP, 1 mM UTP, and or 1 mM modified UTP **3**, 20 μM ATP, 5 μCi α-^{32}P ATP, and 3 U/μL T7 RNA polymerase in a total volume of 20 μL. After 3.5 h at 37 °C, reactions were quenched by adding 20 μL of the loading buffer (7 M urea in 10 mM Tris-HCl, 100 mM EDTA, 0.05% bromophenol blue, pH 8), heated to 75 °C for 3 min, and cooled on an ice bath. The samples (4 μL) were loaded onto a sequencing 18% denaturing polyacrylamide gel and run at a constant power of 11 W for nearly 4 h. The gel was phosphorimaged and the bands were then quantified using the software (GeneTools from Syngene). Percentage incorporation of triphosphate **3** into full-length transcripts was calculated by comparing the transcription efficiency in the presence of natural NTPs. All reactions were performed in duplicate and errors in yields were ±2%.

*Large-Scale Synthesis of Oligoribonucleotides **4**, **5**, and **11** by Transcription Reactions.* Large-scale transcription reactions using template **T1** were performed in a 250 μL reaction volume under similar conditions as mentioned above to isolate control unmodified (**4**) and modified (**5**) oligoribonucleotides. Reactions were performed in the presence of 2 mM GTP, 2 mM CTP, 2 mM ATP, 2 mM UTP, or 2 mM modified UTP **3**, 20 mM $MgCl_2$, 0.4 U/μLRNase inhibitor (RiboLock), 300 nM annealed promoter-template DNA duplex, and 800 units T7 RNA polymerase. After incubation for 12 h at 37 °C, the precipitated salt of pyrophosphate was removed by centrifugation and the reaction volume was reduced approximately to 1/3 by SpeedVac, and 50 μL of loading buffer was added. The mixture was heated at 75 °C for 3 min and cooled on an ice bath. The sample was loaded onto a preparative denaturing polyacrylamide gel (20%) and was electrophoresed under denaturing conditions. The gel was UV shadowed and the appropriate band was excised. The oligoribonucleotide was extracted with 0.3 M sodium acetate and desalted using Sep-Pak classic C18 cartridge. Selenophene-modified A-site oligoribonucleotide **11** was synthesized by following the above procedure using a DNA template sequence 5′ GGTGTGACGCCTATAGTGAGTCGTATTA 3′. Large-scale transcription reactions under these conditions gave nearly 10−16 nmol of the oligoribonucleotide products. Transcript **4**, ε_{260} = 91 000 $M^{-1}cm^{-1}$; transcript **5**, ε_{260} = 91 800 $M^{-1}cm^{-1}$, transcript **11**, ε_{260} = 100 500 $M^{-1}cm^{-1}$.

Enzymatic Digestion of Modified Oligoribonucleotide 5. 3.5 nmol of the modified transcript **5** was treated with snake venom phosphodiesterase I (0.01 U), calf intestinal alkaline phosphatase (10 μL, 1 U/μL), and RNase A (0.25 μg) in a total volume of 100 μL in 50 mM Tris-HCl buffer (pH 8.5, 40 mM $MgCl_2$, 0.1 mM EDTA) for 12 h at 37 °C. RNase T1 (0.2 U/μL) was then added to the above reaction solution and was incubated for another 4 h at 37 °C. The ribonucleoside mixture obtained from the digest was analyzed by RP-HPLC using Eclipse plus C18 column (250 × 4.6 mm, 5 μm) at 260 nm. Mobile phase A: 50 mM triethylammonium acetate buffer (pH 7.5), mobile phase B: acetonitrile. Flow rate: 1 mL/min. Gradient: 0−10% B (10 min), 10−100% B (20 min), and 100% B (10 min). The fractions corresponding to individual ribonucleosides were collected and analyzed by mass spectroscopy. See Table S2 for mass data.

Photophysical Characterization of Oligoribonucleotide 5 and Duplexes of 5. *Steady-State Fluorescence.* Oligoribonucleotide **5** (10 μM) was annealed to custom DNA and RNA ONs (**6**−**10**, 11 μM) by heating ONs in 20 mM cacodylate buffer (pH 7.1, 500 mM NaCl, 0.5 mM EDTA) at 90 °C for 3 min and cooling the samples slowly to room temperature, followed by incubating the solutions in crushed ice. Samples were diluted to give a final concentration of 1 μM (with respect to **5**) in cacodylate buffer. Fluorescently modified duplex constructs were excited at 330 nm with an excitation slit width of 10 nm and emission slit width of 12 nm. Fluorescence experiments were performed in duplicate in a micro fluorescence cell.

Fluorescence Binding Assay. *Fluorescently Modified A-Site RNA Construct **11**•**12**.* For binding experiments, A-site construct (4 μM) **11**•**12** was formed by heating a 1:1 mixture of RNA ONs in HEPES buffer (20 mM HEPES, 100 mM NaCl, 0.5 mM EDTA, pH 7.5) at 75 °C for 5 min. The sample was cooled to RT and placed on crushed ice for ∼4 h. The samples were brought to RT before fluorescence experiments were performed.

*Binding of Aminoglycosides to a Model Selenophene-Modified A-Site RNA **11**•**12**.* Aliquots (1 μL) of increasing concentrations of the aminoglycoside stock was added to a micro fluorescence cuvette containing 200 μL of A-site construct **11**•**12** (4 μM) in the above HEPES buffer. The fluorescence spectrum after each addition of the aminoglycoside was recorded by exciting at 330 nm with excitation and emission slit widths of 6 and 8 nm, respectively. The aminoglycoside was added till fluorescence saturation was

dx.doi.org/10.1021/bc400194g | *Bioconjugate Chem.* 2013, 24, 1367−1377

observed. The change in volume over the entire titration was ≤8%. A spectral blank of the HEPES buffer in the absence of RNA and aminoglycoside was subtracted from all titrations. All fluorescence titrations were performed in triplicate. Normalized fluorescence intensity (F_N) versus log of aminoglycoside (AG) concentration plots were fitted using eq 1 (KaleidaGraph) to determine the EC_{50} values for the binding of aminoglycosides to A-site construct.[53,54]

$$F_N = \frac{F_i - F_0}{F_s - F_0}$$

F_i is the fluorescence intensity at each titration point. F_0 and F_s are the fluorescence intensity in the absence of aminoglycoside and at saturation, respectively. n is the Hill coefficient or degree of cooperativity associated with the binding.

$$F_N = F_0 + \left(\frac{F_s[\mathrm{AG}]^n}{[\mathrm{EC}_{50}]^n + [\mathrm{AG}]^n} \right) \quad (1)$$

RESULTS AND DISCUSSION

Synthesis and Photophysical Properties of Selenophene-Modified Uridine. The selenophene-modified uridine analog **2** has been synthesized by reacting 5-iodouridine **1** with 2-(tri-*n*-butylstannyl)selenophene under typical Stille cross-coupling reaction conditions using a palladium catalyst, $Pd(PPh_3)_2Cl_2$ (Scheme 1). Many fluorescence probes that have been used to study the structure and function of nucleic acids photophysically respond to changes in their surrounding environment (e.g., polarity and viscosity).[15] The ground-state electronic spectrum of nucleoside **2** in various solvents shows two major absorption maxima, which is not significantly affected by solvent polarity changes (Figure 1 and Table 1). However, fluorescence properties such as quantum yield, emission maximum, and excited-state lifetime are significantly affected by polarity changes. In water, the nucleoside has an emission band centered around 454 nm, which significantly blue shifts (17 nm) and also shows a hyperchromic effect (~2-fold) as the solvent polarity is decreased from water to dioxane (Figure 1, Table 1). The time-resolved fluorescence spectroscopy analysis reveals a longer lifetime in water, which decreases in less polar solvents (Table 1 and Figure S1). A positive correlation is obtained when the Stokes shift in different solvents is plotted as a function of $E_T(30)$, Reichardt's microscopic solvent polarity parameter, which further indicates that the nucleoside **2** is sensitive to its microenvironment (Figure S2).[56]

Scheme 1. Synthesis of Selenophene-Modified Uridine Analog 2 and Corresponding Triphosphate 3[55a]

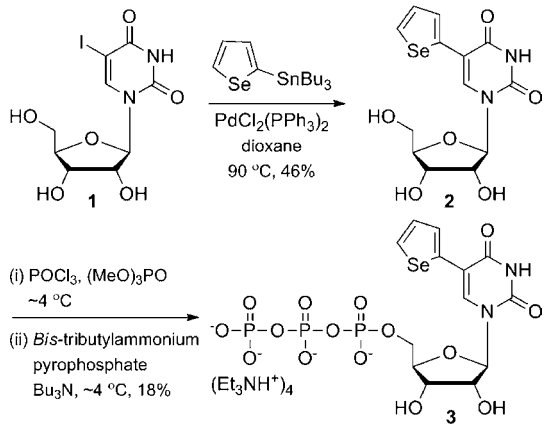

[a]2-(Tributylstannyl)selenophene was synthesized by following a literature report.[51]

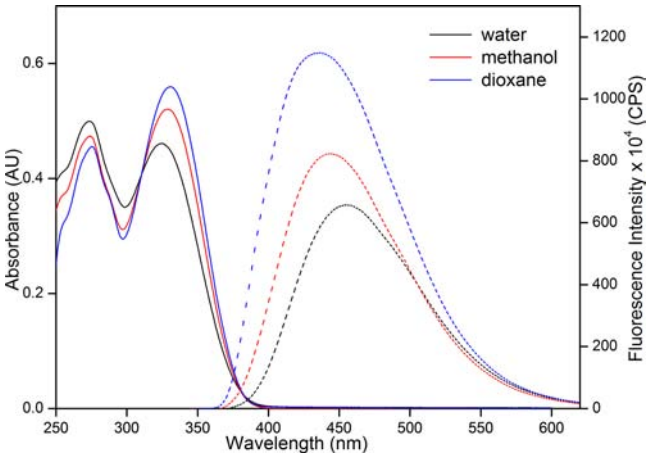

Figure 1. Absorption (solid line, 50 μM) and emission (dashed line, 5 μM) spectra of nucleoside **2** in different solvents.[55]

Table 1. Photophysical Properties of 2 in Different Solvents[55]

solvent	λ_{max}[a] (nm)	λ_{em} (nm)	I_{rel}[b]	Φ[c]	τ_{av}[c] (ns)
water	325	454	1.00	0.014	0.40
methanol	329	445	1.25	0.015	0.23
dioxane	331	437	1.75	0.025	0.27

[a]The lowest energy maximum is given. [b]Fluorescence intensity with respect to intensity in water. [c]Standard deviations for quantum yield (Φ) and average lifetime (τ_{av}) are ≤0.001 and 0.01 ns, respectively.

The conformation of selenophene moiety with respect to pyrimidine ring connected by a rotatable aryl−aryl bond can affect the effective conjugation and, hence, the fluorescence properties of the emissive nucleoside. The conformation of such extended nucleoside analogs, when incorporated into ONs, can be affected by subtle changes in interaction with neighboring bases during a folding or recognition process.[57] In order to evaluate if nucleoside **2** could be utilized as a conformation-sensitive probe, further photophysical characterization has been carried out in solvents of similar polarity but different viscosity. Upon excitation, the nucleoside in glycerol shows a nearly 2-fold enhancement in fluorescence intensity with no apparent change in the emission maximum as compared to in a less viscous medium, ethylene glycol (Figure 2 and Table S1). Furthermore, excited-state decay kinetics and fluorescence anisotropy analysis indicate a longer lifetime and a higher anisotropy value in glycerol than in ethylene glycol due to rigidification of the fluorophore in a more viscous medium (Table S1). This dual-sensitivity of the nucleoside to polarity and viscosity changes, which bestows probe-like character to the nucleoside, encouraged us to incorporate the fluorescent nucleoside **2** into RNA ONs.

Enzymatic Incorporation of Selenophene-Modified UTP Analog. Modified RNA ONs can be obtained by solid-phase chemical synthesis and by enzymatic methods using RNA polymerases and ligases.[49,58−61] Here, we have adopted in vitro transcription reactions in the presence of T7 RNA polymerase,

dx.doi.org/10.1021/bc400194g | Bioconjugate Chem. 2013, 24, 1367−1377

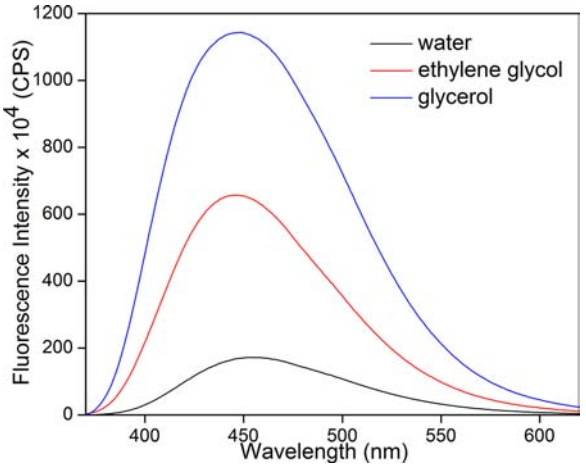

Figure 2. Emission spectra of nucleoside **2** (5 μM) in solvents of different viscosity.[55]

similar to Tor's report,[49] to incorporate the selenophene-modification into RNA ONs. Selenophene-modified UTP **3** necessary for transcription reactions has been prepared in two steps by treating nucleoside **2** with $POCl_3$ and then with *bis*-tributylammonium pyrophosphate (Scheme 1).[49,62] Transcription reactions have been carried out in the presence of a series of promoter-template DNA duplexes constructed by hybridizing a promoter DNA sequence with DNA templates **T1**–**T5** (Figure 3). The templates contain one or two dA

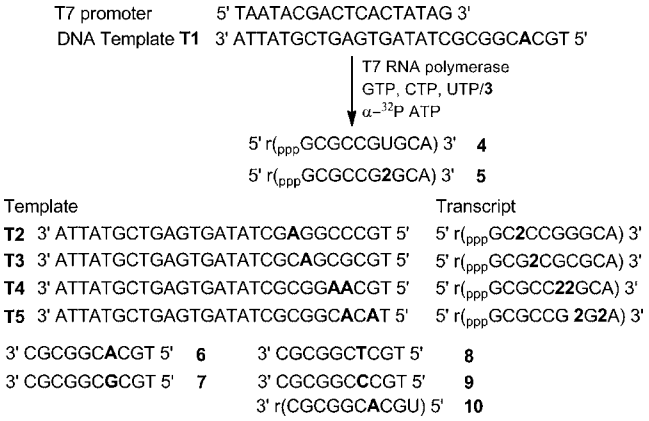

Figure 3. Synthesis of selenophene-modified fluorescent RNA ONs by in vitro transcription reactions in the presence of DNA templates **T1**–**T5**. cDNA (**6**–**9**) and cRNA (**10**) ONs used in this study.[55]

residues to facilitate single or double incorporations of the monophosphate of **3** into RNA transcripts. In addition, all templates contain a dT residue at the 5′-end to guide the incorporation of a unique adenosine residue at the 3′-end of each transcript. Therefore, in a transcription reaction (in the presence of GTP, CTP, **3**, and α-^{32}P ATP), if T7 RNA polymerase accepts and incorporates the modification then the full-length modified RNA product would contain a ^{32}P-labeled adenosine at the 3′-end, which could be resolved on a polyacrylamide gel and phosphorimaged. However, abortive sequences resulting from failed transcription reactions would not carry the radiolabel, and hence, would remain undetected in this reaction setup.

A transcription reaction carried out in the presence of template **T1** and triphosphate **3** afforded the full-length RNA ON **5** containing selenophene-modified uridine at the +7 position in a very good yield (Figure 4, lane 2). In addition to

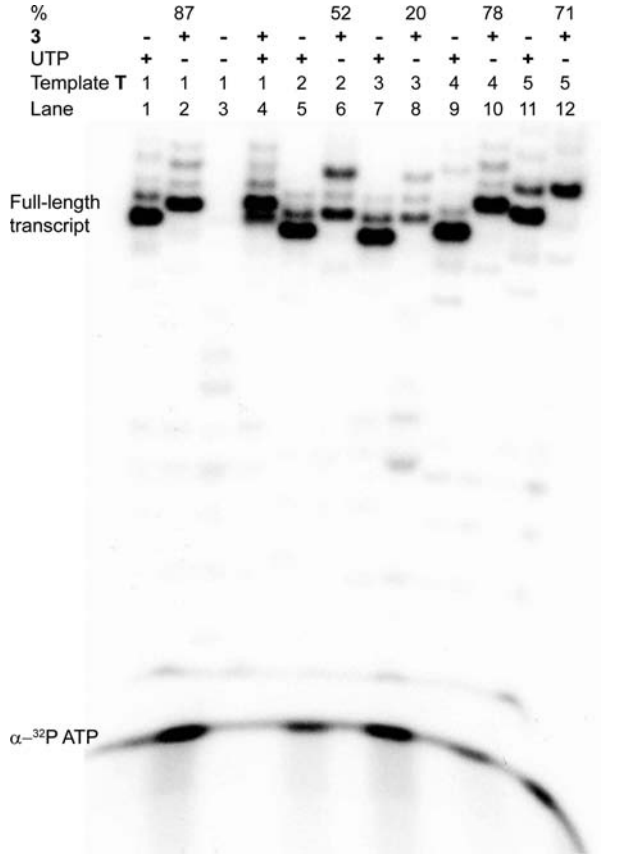

Figure 4. PAGE of transcription products from in vitro transcription reactions with DNA templates **T1**–**T5** in the presence of UTP and modified UTP **3** under denaturing conditions. % incorporation of **3** into the full-length oligoribonucleotide product is reported with respect to the amount of full-length product formed in the presence of natural UTP.[55]

the full-length product, trace amounts of random nontemplated incorporation products (N+1 and N+2) are also formed. Such nontemplated incorporation products are known to form in trace amounts in in vitro transcription reactions.[63] Absence of bands corresponding to full-length transcripts in a control reaction performed in the absence of UTP and **3** rules out any adventitious misincorporation (Figure 4, lane 3). Interestingly, RNA polymerase incorporates the modified UTP better as compared to the natural UTP in a reaction containing equimolar concentrations of **3** and UTP (Figure 4, lane 4). Reactions in the presence of templates **T2** and **T3** result in the formation of transcripts containing the modification near the promoter region (+3 and +4 positions, respectively) in lower yields (Figure 4, lanes 6 and 8), whereas when reactions are performed in the presence of templates **T4** and **T5**, the polymerase produces doubly modified transcripts in good yields (Figure 4, lanes 10 and 12).

The fluorescently modified oligoribonucleotide **5** was isolated from large-scale transcription reactions for further chemical and photophysical characterizations. MALDI-TOF mass analysis gave the mass corresponding to the full-length modified oligoribonucleotide product **5** (Figure S3). Furthermore, HPLC analysis of the authentic ribonucleoside samples

dx.doi.org/10.1021/bc400194g | *Bioconjugate Chem.* 2013, 24, 1367–1377

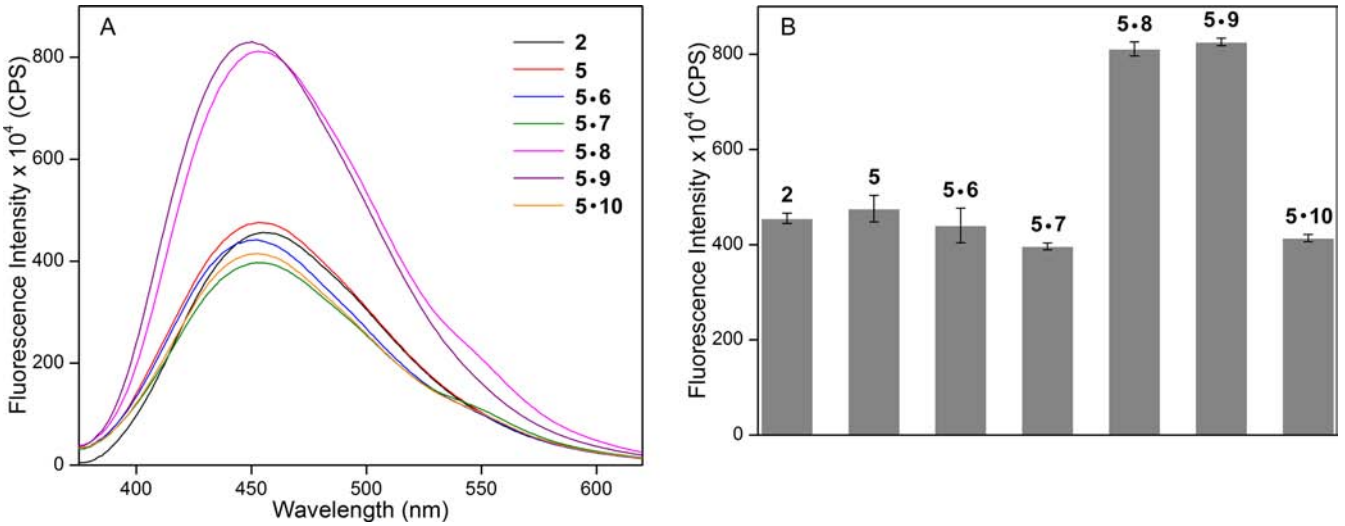

Figure 5. (A) Emission spectra (1 μM) of nucleoside **2**, ON **5**, and duplexes made by hybridizing **5** with complementary (**6** and **10**) and mismatched (**7**–**9**) ONs. (B) Fluorescence intensity of **5** and duplexes made of **5** at 452 nm.[55]

and ribonucleoside products obtained from enzymatic digestion of **5** clearly ascertained the presence of selenophene-modified nucleoside in the transcription product (Figure S4). Although the selenophene moiety attached at the 5-position of uracil is reasonably small, its incorporation can potentially affect the native structure of oligoribonucleotides and their ability to form stable duplexes. Small differences in T_m values (ΔT_m = ~3 °C) between control unmodified (**4•6** and **4•10**) and modified (**5•6** and **5•10**) duplexes indicate that the modification has only a minor impact on the duplex stability (Figure 3 and Figure S5). Collectively, these results highlight that in vitro transcription reaction catalyzed T7 RNA polymerase can be used as a viable method to incorporate the minimally perturbing fluorescent selenophene-modified nucleoside into RNA ONs.

Selenophene-Modified Uridine Analog in Different Base Environment. It is observed that the photophysical properties of the majority fluorescent nucleoside analogs, when incorporated into ONs, are affected by various mechanisms, which often involve neighboring nucleobases.[57,64−68] Hence, the photophysical behavior of fluorescent nucleoside **2** in different base environments has been studied by steady-state and time-resolved fluorescence spectroscopic techniques using transcript **5** and duplexes made by hybridizing **5** with complementary DNA and RNA ONs (**6**−**10**, Figure 3). The duplexes have been designed in such a fashion that the selenophene-modified ribonucleoside **2** has been positioned opposite to complementary or mismatched bases. When excited at 330 nm, a solution of single stranded oligoribonucleotide **5** in cacodylate buffer displays an emission band similar to that of the free nucleoside **2** (Figure 5A and B). RNA−DNA duplex **5•6** and RNA−RNA duplex **5•10** in which the ribonucleoside **2** is placed opposite the complementary bases, dA and A, respectively, show emission profiles analogous to the single stranded oligoribonucleotide **5**. Interestingly, **2** placed opposite the pyrimidine bases in duplexes **5•8** and **5•9** shows a nearly 2-fold enhancement in fluorescence intensity as compared to duplexes **5•6** and **5•7** in which **2** is placed opposite the purines (Figure 5A and B). This observation is noteworthy because, baring a few examples,[48,69−71] the majority of fluorescent nucleoside analog probes when incorporated into single stranded and double stranded ONs display sequential quenching in fluorescence intensity due to stacking of the chromophore with flanking bases and/or electron transfer process.[64−66,72]

Although the exact morphology of emissive nucleoside in these duplexes is unknown, the enhancement in fluorescence intensity exhibited by **2** when placed opposite the pyrimidines can possibly be due to the following reasons. It is likely in duplexes **5•6** and **5•7** that the fluorescent uridine analog is locked due to the formation of a stable Watson−Crick and a wobble base pair with dA and dG residues, respectively. This would favor the nonradiative decay pathway due to electron transfer process between nucleoside **2** and neighboring bases.[72] However, in duplexes **5•8** and **5•9** the emissive nucleoside is opposite the mismatched bases dT and dC, respectively, and hence is not constrained by H-bonding interactions. This could reduce the electron transfer between the selenophene-modified base and neighboring bases. The relative conformation of the selenophene moiety and uracil ring, which could be affected by interactions with neighboring bases, could also contribute to the overall photophysical behavior of the nucleoside in different base environments.[57] Excited-state decay kinetics show longer lifetimes for **5•8** and **5•9** as compared to **5•6** and **5•7**, which further suggest that the microenvironment of emissive nucleoside in this set of duplexes is distinctly different (Figure S6 and Table S3). Taken together, these observations clearly indicate that the fluorescence properties of nucleoside **2** are affected by base pair substitution. Such environmentally sensitive fluorescent nucleoside analogs that report subtle alterations in their neighboring base environment during a recognition event have been utilized in devising assays to study the dynamics, structure, and binding properties of nucleic acids.[15−17]

Fluorescence Detection of Aminoglycoside Antibiotics Binding to A-Site RNA. To explore the usefulness of selenophene-modified uridine **2** in investigating the recognition property of RNA, we have chosen a therapeutically important and well-studied RNA motif, bacterial ribosomal decoding site (A-site), as a test system.[73,74] The A-site RNA maintains the high fidelity of protein translation process by monitoring correct mRNA codon and tRNA anticodon base

pairing.[75] An important component of the decoding center is a small loop present in the 16S rRNA, which contains flexible adenine residues A1492 and A1493 (Figure 6A). Naturally occurring aminoglycoside antibiotics (e.g., paromomycin and neomycin) bind to this region of the bacterial 16S rRNA and fix A1492 and A1493 in a conformation similar to the one induced by cognate tRNA binding to the A-site (Figure S7).[76,77] This reduces the ability of bacterial A-site to discriminate between the correct and incorrect codon−anticodon pairs resulting in mistranslation.

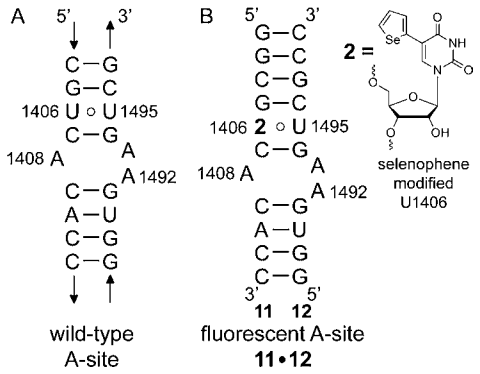

Figure 6. (A) Secondary structure of the bacterial A-site motif that binds to aminoglycoside antibiotics. (B) Selenophene-modified fluorescent A-site model construct **11•12** used in this study.[55]

Based on the structures of aminoglycosides complexed with A-site,[78,79] fluorescent A-site RNA surrogates have been constructed by replacing A1492 or A1493 or U1406 residues with fluorescent nucleoside analogs.[49,53,80−84] These constructs have been used in determining the binding constants and thermodynamic parameters of A-site−aminoglycoside complexes by monitoring the changes in the fluorescence properties. Although reasonably sensitive, the fluorescence response of some of these analogs (e.g., 2-aminopurine (2-AP)) is aminoglycoside-specific.[49,53,83,84] Therefore, robust assays that are amicable to discovery platforms for the identification of new bacterial-specific RNA binders are highly desired to counter the ever increasing number of antibiotic-resistant strains.

Encouraged by crystal structures showing evidence for further stabilization of A-site−aminoglycoside complexes through direct and water-bridged H-bonds to the non-canonical U1406∘U1495 pair,[78,79] we decided to replace one of the uridine residues (U1406) with selenophene-modified uridine analog **2** to generate a fluorescent A-site RNA construct. To synthesize the fluorescent A-site construct by in vitro transcription reactions, we chose a short RNA duplex (**11•12**) that essentially represents the aminoglycosides binding domain of the wild type A-site (Figure 6B).[49,53,81−84] Oligoribonucleotide **11** containing emissive ribonucleoside **2** at U1406 was synthesized by large-scale transcription reactions in the presence of triphosphate **3**. The integrity of the modified full-length transcript was confirmed by mass analysis (Figure S3). The fluorescent A-site construct was assembled by hybridizing **11** with a custom synthesized counter strand **12** in HEPES buffer. The A-site construct was excited at 330 nm and changes in fluorescence intensity upon titration with aminoglycosides were recorded at its emission maximum 452 nm. Titration of paromomycin to **11•12** resulted in an increase in fluorescence intensity, which corresponded to a nearly 2-fold at the saturation concentration of the aminoglycoside (Figure 7A). An EC_{50} value (concentration required for 50% response) of 7.57 ± 0.10 μM for the titration of paromomycin to A-site was found to be in good agreement with earlier literature reports (Figure 7B).[53,81−84]

2-AP, a widely used fluorescent adenosine analog, has been previously employed in constructing A-site RNA motifs by replacing either A1492 or A1493 residues.[53,83,84] While 2-AP-modified A-site constructs photophysically report the binding of paromomycin, they fail to signal the binding of neomycin (Figure S8).[49,53,83,84] This observation is particularly intriguing because the structures of A-site complexed with paromomycin and neomycin closely resemble each other.[78,79] To test if selenophene-modified uridine **2** could photophysically report the binding of neomycin to A-site, duplex **11•12** was titrated

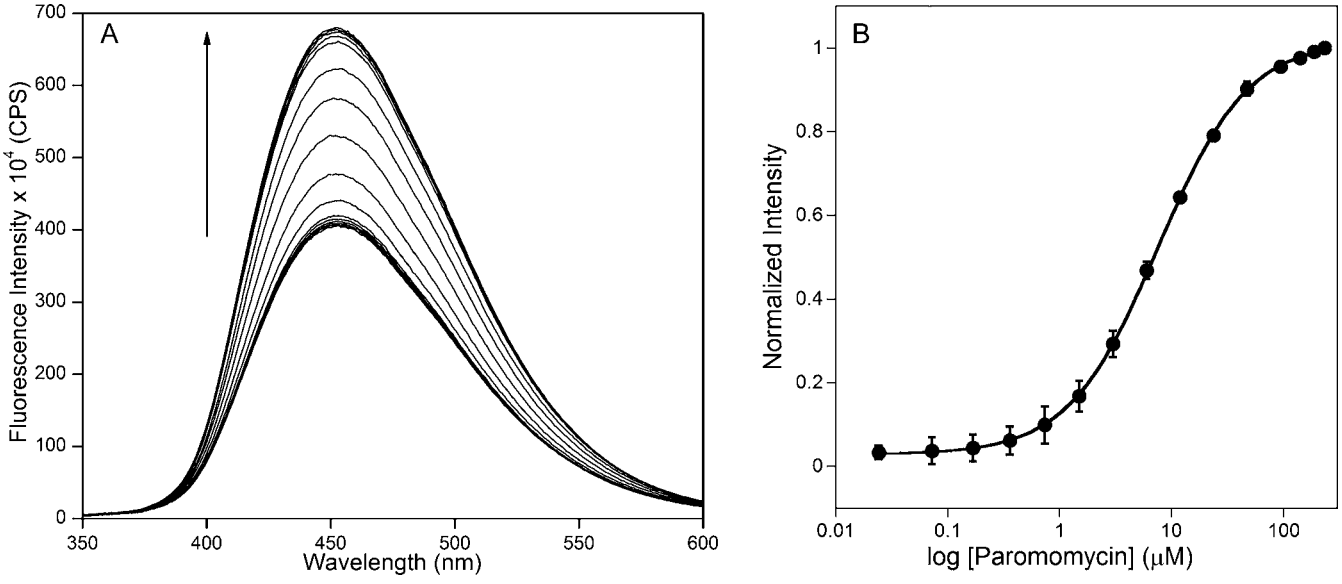

Figure 7. (A) Emission spectra for the titration of A-site construct **11•12** with paromomycin. (B) Curve fit for the titration of A-site with paromomycin. Normalized fluorescence intensity at λ_{em} = 452 nm is plotted against log [aminoglycoside]. Hill coefficient (n) = 1.1.[55]

dx.doi.org/10.1021/bc400194g | Bioconjugate Chem. 2013, 24, 1367−1377

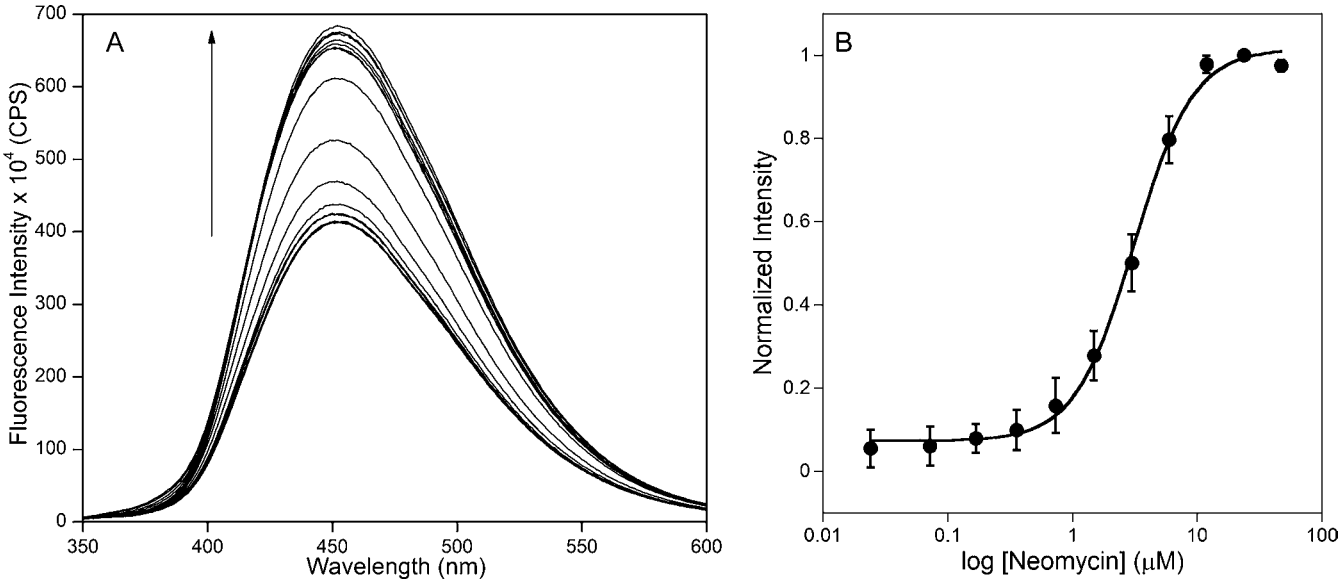

Figure 8. (A) Emission spectra for the titration of A-site construct **11**•**12** with neomycin. (B) Curve fit for the titration of A-site with neomycin. Normalized fluorescence intensity at λ_{em} = 452 nm is plotted against log [aminoglycoside]. Hill coefficient (n) = 1.8.[55]

with neomycin B. Rewardingly, the emissive nucleoside signaled the binding of neomycin to A-site construct with enhancement in fluorescence intensity, which corresponded to a comparable EC_{50} value of 3.13 ± 0.17 μM (Figure 8A and B).[49] Importantly, control titrations performed by titrating single stranded ON **11** with either paromomycin or neomycin resulted in minor changes in fluorescence intensity (Figure S9). This indicates that the increase in fluorescence intensity exhibited by nucleoside **2** is due to cognate binding of aminoglycosides to A-site construct **11**•**12**. A furan-modified fluorescent A-site RNA construct developed by Tor's group also signals the binding of paromomycin and neomycin with enhancement in fluorescence intensity.[49] However, the EC_{50} values for the binding of paromomycin and neomycin to A-site (11.5 μM and 5.0 μM, respectively) determined by using furan-modified A-site were found to be higher than the literature reports.[49,53,81−84] On the other hand, selenophene-modified nucleoside **2** reports the binding of aminoglycoside antibiotics to bacterial decoding site with EC_{50} values closer to literature reports. Taken together, these results clearly demonstrate that the selenophene-modified nucleoside **2** is a useful probe in detecting RNA−ligand interactions, in this case A-site−aminoglycoside complexes, which cannot be effectively monitored by 2-AP, a most commonly used probe for studying RNA−ligand interactions. Importantly, this heavy-atom-containing nucleoside has a clear advantage over many other fluorescence probes as it can be used to investigate the nucleic acid structure and function in real time by fluorescence as well as in solid state by X-ray crystallography.

CONCLUSIONS

We have developed a new ribonucleoside analog probe **2** by appending selenophene moiety at the 5-position of uridine. The emissive nucleoside exhibits favorable photophysical properties such as sensitivity to changes in its microenvironment and conformation. The amicability of modified ribonucleotide to enzymatic incorporation has allowed the easy synthesis of a selenophene-modified fluorescent A-site RNA construct by transcription reaction. Our results demonstrate that the selenophene-modified uridine incorporated into the decoding site can effectively signal the binding of aminoglycoside antibiotics to the bacterial A-site. Taken together, this heavy-atom containing fluorescent label is a unique and useful combination wherein its dual properties can be utilized to study the dynamics, structure, and recognition properties of nucleic acids by two mutually exclusive but complementing techniques, namely, fluorescence and X-ray crystallography. We strongly believe that this simple approach of assembling a "two-in-one" probe would provide new opportunities to study the structure−function relationship of biomacromolecules. Efforts to incorporate and crystallize selenophene-modified DNA and RNA motifs of biological relevance are currently in progress.

ASSOCIATED CONTENT

Supporting Information

Experimental procedures, Figure S1−S9, Table S1−S3, and NMR spectra. This material is available free of charge via the Internet at http://pubs.acs.org.

AUTHOR INFORMATION

Corresponding Author

*E-mail: srivatsan@iiserpune.ac.in.

Notes

The authors declare no competing financial interest.

ACKNOWLEDGMENTS

S.G.S is grateful to the Department of Science and Technology, India (SR/S1/OC-51/2009) and Council of Scientific and Industrial Research (CSIR), India (02-0086/12/EMR-II) for research grants. M.G.P. and A.N. thank CSIR for graduate research fellowship.

ABBREVIATIONS

ON, oligonucleotide; SAD, single-wavelength anomalous dispersion; MAD, multiwavelength anomalous dispersion; RP, reversed-phase; TEAB, triethylammonium bicarbonate buffer; AG, aminoglycoside; 2-AP, 2-aminopurine

REFERENCES

(1) Hermann, T., and Patel, D. J. (2000) RNA bulges as architectural and recognition motifs. *Structure 8*, R47−R54.

(2) Leulliot, N., and Varani, G. (2001) Current topics in RNA-Protein recognition: control of specificity and biological function through induced fit and conformational capture. *Biochemistry 40*, 7947−7956.

(3) Al-Hashimi, H. M., and Walter, N. G. (2008) RNA dynamics: it is about time. *Curr. Opin. Struct. Biol. 18*, 321−329.

(4) Aitken, C. E., Petrov, A., and Puglisi, J. D. (2010) Single ribosome dynamics and the mechanism of translation. *Annu. Rev. Biophys. 39*, 491−513.

(5) Ranasinghe, R. T., and Brown, T. (2005) Fluorescence based strategies for genetic analysis. *Chem. Commun.*, 5487−5502.

(6) Asseline, U. (2006) Development and application of fluorescent oligonucleotides. *Curr. Org. Chem. 10*, 491−518.

(7) Martí, A. A., Jockusch, S., Stevens, N., Ju, J., and Turro, N. J. (2007) Fluorescent hybridization probes for sensitive and selective DNA and RNA detection. *Acc. Chem. Res. 40*, 402−409.

(8) Bardaro, M. F., Jr., and Varani, G. (2012) Examining the relationship between RNA function and motion using nuclear magnetic resonance. *WIREs RNA 3*, 122−132.

(9) Nguyen, P., and Qin, P. Z. (2012) RNA dynamics: perspectives from spin labels. *WIREs RNA 3*, 62−72.

(10) Holbrook, S. R. (2008) Structural principles from large RNAs. *Annu. Rev. Biophys. 37*, 445−464.

(11) Serganov, A., and Patel, D. J. (2012) Molecular recognition and function of riboswitches. *Curr. Opin. Struct. Biol. 22*, 279−286.

(12) Weisbrod, S. H., and Marx, A. (2008) Novel strategies for the site-specific covalent labelling of nucleic acids. *Chem. Commun.*, 5675−5685.

(13) Wachowius, F., and Höbartner, C. (2010) Chemical RNA modifications for studies of RNA structure and dynamics. *ChemBioChem 11*, 469−480.

(14) Khakshoor, O., and Kool, E. T. (2011) Chemistry of nucleic acids: impacts in multiple fields. *Chem. Commun. 47*, 7018−7024.

(15) Sinkeldam, R. W., Greco, N. J., and Tor, Y. (2010) Fluorescent analogs of biomolecular building blocks: design, properties, and applications. *Chem. Rev. 110*, 2579−2619.

(16) Wilhelmsson, L. M. (2010) Fluorescent nucleic acid base analogues. *Quart. Rev. Biophy. 43*, 159−183.

(17) Srivatsan, S. G., and Sawant, A. A. (2011) Fluorescent ribonucleoside analogues as probes for investigating RNA structure and Function. *Pure Appl. Chem. 83*, 213−232.

(18) Phelps, K., Morris, A., and Beal, P. A. (2012) Novel modifications in RNA. *ACS Chem. Biol. 7*, 100−109.

(19) Teo, Y. N., and Kool, E. T. (2012) DNA-multichromophore systems. *Chem. Rev. 112*, 4221−4245.

(20) Förster, U., Lommel, K., Sauter, D., Grünewald, C., Engels, J. W., and Wachtveitl, J. (2010) 2-(1-Ethynylpyrene)-adenosine as a folding probe for RNA—pyrene in or out. *ChemBioChem 11*, 664−672.

(21) Peacock, H., Maydanovych, O., and Beal, P. A. (2010) N^2-modified 2-aminopurine ribonucleosides as minor-groove-modulating adenosine replacements in duplex RNA. *Org. Lett. 12*, 1044−1047.

(22) Kimoto, M., Mitsui, T., Yokoyama, S., and Hirao, I. (2010) A unique fluorescent base analogue for the expansion of the genetic alphabet. *J. Am. Chem. Soc. 132*, 4988−4989.

(23) Nadler, A., Strohmeier, J., and Diederichsen, U. (2011) 8-Vinyl-2′-deoxyguanosine as a fluorescent 2′-deoxyguanosine mimic for investigating DNA hybridization and topology. *Angew. Chem., Int. Ed. 50*, 5392−5396.

(24) Ehrenschwender, T., and Wagenknecht, H.-A. (2011) 4,4-Difluoro-4-bora-3a,4a-diaza-s-indacene as a bright fluorescent label for DNA. *J. Org. Chem. 76*, 2301−2304.

(25) Lee, J., II., and Kim, B. H. (2012) Monitoring i-motif transitions through the exciplex emission of a fluorescent probe incorporating two PyA units. *Chem. Commun. 48*, 2074−2076.

(26) Wojciechowski, F., Lietard, J., and Leumann, C. J. (2012) 2-Pyrenyl-DNA: synthesis, pairing, and fluorescence properties. *Org. Lett. 14*, 5176−5179.

(27) Halogenated ONs are light sensitive and undergo dehalogenation when exposed to X−ray radiation, which cause failures in phasing; Ennifar, E., Carpentier, P., Ferrer, J.-L., Walter, P., and Dumas, P. (2002) X-ray-induced debromination of nucleic acids at the Br *K* absorption edge and implications for MAD Phasing. *Acta Crystallogr. D58*, 1262−1268.

(28) Dibrov, S., Mclean, J., and Hermann, T. (2011) Structure of an RNA dimer of a regulatory element from human thymidylate synthase mRNA. *Acta Crystallogr. D67*, 97−104.

(29) Egli, M., and Pallan, P. S. (2007) Insights from crystallographic studies into the structural and pairing properties of nucleic acid analogs and chemically modified DNA and RNA oligonucleotides. *Annu. Rev. Biophys. Biomol. Struct. 36*, 281−305.

(30) Sheng, J., and Huang, Z. (2010) Selenium derivatization of nucleic acids for X-Ray crystal-structure and function studies. *Chem. Biodivers. 7*, 753−785.

(31) Du, Q., Carrasco, N., Teplova, M., Wilds, C. J., Egli, M., and Huang, Z. (2002) Internal derivatization of oligonucleotides with selenium for X-ray crystallography using MAD. *J. Am. Chem. Soc. 124*, 24−25.

(32) Wilds, C. J., Pattanayek, R., Pan, C., Wawrzak, Z., and Egli, M. (2002) Selenium-assisted nucleic acid crystallography: use of phosphoroselenoates for MAD phasing of a DNA structure. *J. Am. Chem. Soc. 124*, 14910−14916.

(33) Teplova, M., Wilds, C. J., Wawrzak, Z., Tereshko, V., Du, Q., Carrasco, N., Huang, Z., and Egli, M. (2002) Covalent incorporation of selenium into oligonucleotides for X-ray crystal structure determination via MAD: proof of principle. *Biochimie 84*, 849−858.

(34) Carrasco, N., Caton-Williams, J., Brandt, G., Wang, S., and Huang, Z. (2006) Efficient enzymatic synthesis of phosphoroselenoate RNA by using adenosine 5′-(α-*P*-seleno)triphosphate. *Angew. Chem., Int. Ed. 45*, 94−97.

(35) Höbartner, C., and Micura, R. (2004) Synthesis of selenium-modified oligoribonucleotides and their enzymatic ligation leading to an U6 SnRNA stem-loop segment. *J. Am. Chem. Soc. 126*, 1141−1149.

(36) Salon, J., Sheng, J., Jiang, J., Chen, G., Caton-Williams, J., and Huang, Z. (2007) Oxygen replacement with selenium at the thymidine 4-position for the Se base pairing and crystal structure studies. *J. Am. Chem. Soc. 129*, 4862−4863.

(37) Caton-Williams, J., and Huang, Z. (2008) Synthesis and DNA-polymerase incorporation of colored 4-selenothymidine triphosphate for polymerase recognition and DNA visualization. *Angew. Chem., Int. Ed. 47*, 1723−1725.

(38) Serganov, A., Keiper, S., Malinina, L., Tereshko, V., Skripkin, E., Höbartner, C., Polonskaia, A., Phan, A. T., Wombacher, R., Micura, R., Dauter, Z., Jäschke, A., and Patel, D. J. (2005) Structural basis for Diels-Alder ribozyme-catalyzed carbon-carbon bond formation. *Nat. Struct. Mol. Biol. 12*, 218−224.

(39) Freisz, S., Lang, K., Micura, R., Dumas, P., and Ennifar, E. (2008) Binding of aminoglycoside antibiotics to the duplex form of the HIV-1 genomic RNA dimerization initiation site. *Angew. Chem., Int. Ed. 47*, 4110−4113.

(40) Salon, J., Jiang, J., Sheng, J., Gerlits, O. O., and Huang, Z. (2008) Derivatization of DNAs with selenium at 6-position of guanine for function and crystal structure studies. *Nucleic Acids Res. 36*, 7009−7018.

(41) Olieric, V., Rieder, U., Lang, K., Serganov, A., Schulze-Briese, C., Micura, R., Dumas, P., and Ennifar, E. (2009) A fast selenium derivatization strategy for crystallization and phasing of RNA structures. *RNA 15*, 707−715.

(42) Sun, H., Sheng, J., Hassan, A. E. A., Jiang, S., Gan, J., and Huang, Z. (2012) Novel RNA base pair with higher specificity using single selenium atom. *Nucleic Acids Res. 40*, 5171−5179.

(43) Wahba, A. S., Esmaeili, A., Damha, M. J., and Hudson, R. H. E. (2010) A single-label phenylpyrrolocytidine provides a molecular

beacon-like response reporting HIV-1 RT RNase H activity. *Nucleic Acids Res. 38*, 1048−1056.
(44) Shin, D., Sinkeldam, R. W., and Tor, Y. (2011) Emissive RNA alphabet. *J. Am. Chem. Soc. 133*, 14912−14915.
(45) Tanpure, A. A., and Srivatsan, S. G. (2011) A microenvironment-sensitive fluorescent pyrimidine ribonucleoside analogue: synthesis, enzymatic incorporation, and fluorescence detection of a DNA abasic site. *Chem.—Eur. J. 17*, 12820−12827.
(46) Pawar, M. G., and Srivatsan, S. G. (2011) Synthesis, photophysical characterization, and enzymatic incorporation of a microenvironment-sensitive fluorescent uridine analog. *Org. Lett. 13*, 1114−1117.
(47) Riedl, J., Pohl, R., Ernsting, N. P., Orság, P., Fojta, M., and Hocek, M. (2012) Labelling of nucleosides and oligonucleotides by solvatochromic 4-aminophthalimide fluorophore for studying DNA−protein interactions. *Chem. Sci. 3*, 2797−2806.
(48) Tanpure, A. A., and Srivatsan, S. G. (2012) Synthesis and photophysical characterisation of a fluorescent nucleoside analogue that signals the presence of an abasic site in RNA. *ChemBioChem 13*, 2392−2399.
(49) Srivatsan, S. G., and Tor, Y. (2007) Fluorescent pyrimidine ribonucleotide: synthesis, enzymatic incorporation, and utilization. *J. Am. Chem. Soc. 129*, 2044−2053.
(50) Greco, N. J., and Tor, Y. (2005) Simple fluorescent pyrimidine analogues detect the presence of DNA Abasic sites. *J. Am. Chem. Soc. 127*, 10784−10785.
(51) Tributyl(2-selenophene)stannane was prepared by following a literature report. Instead of performing the reaction in dry THF, it was performed in dry diethyl ether at nearly −70 °C. Yang, R., Tian, R., Yan, J., Zhang, Y., Yang, J., Hou, Q., Yang, W., Zhang, C., and Cao, Y. (2005) Deep-red electroluminescent polymers: synthesis and characterization of new low-band-gap conjugated copolymers for light-emitting diodes and photovoltaic devices. *Macromolecules 38*, 244−253.
(52) Moffatt, J. G. (1964) A general synthesis of nucleoside 5′ triphosphates. *Can. J. Chem. 42*, 599−604.
(53) Shandrick, S., Zhao, Q., Han, Q., Ayida, B. K., Takahashi, M., Winters, G. C., Simonsen, K. B., Vourloumis, D., and Hermann, T. (2004) Monitoring molecular recognition of the ribosomal decoding site. *Angew. Chem., Int. Ed. 43*, 3177−3182.
(54) Tam, V. K., Kwong, D., and Tor, Y. (2007) Fluorescent HIV-1 dimerization initiation site: design, properties, and use for ligand discovery. *J. Am. Chem. Soc. 129*, 3257−3266.
(55) See Experimental section for details.
(56) Reichardt, C. (1994) Solvatochromic dyes as solvent polarity indicators. *Chem. Rev. 94*, 2319−2358.
(57) Fluorescence properties of fluorophores containing a molecular rotor element are affected by molecular crowing effects and viscosity. Sinkeldam, R. W., Wheat, A. J., Boyaci, H., and Tor, Y. (2011) Emissive nucleosides as molecular rotors. *ChemPhysChem 12*, 567−570.
(58) Rieder, R., Lang, K., Graber, D., and Micura, R. (2007) Ligand-induced folding of the adenosine deaminase A-riboswitch and implications on riboswitch translational control. *ChemBioChem 8*, 896−902.
(59) Hikida, Y., Kimoto, M., Yokoyama, S., and Hirao, I. (2010) Site-specific fluorescent probing of RNA molecules by unnatural base-pair transcription for local structural conformation analysis. *Nat. Protoc. 5*, 1312−1323.
(60) Kimoto, M., Mitsui, T., Harada, Y., Sato, A., Yokoyama, S., and Hirao, I. (2007) Fluorescent probing for RNA molecules by an unnatural base-pair system. *Nucleic Acids Res. 35*, 5360−5369.
(61) Rao, H., Tanpure, A. A., Sawant, A. A., and Srivatsan, S. G. (2012) Enzymatic incorporation of an azide-modified UTP analog into oligoribonucleotides for post-transcriptional chemical functionalization. *Nat. Protoc. 7*, 1097−1112.
(62) Ludwig, J. (1981) A new route to nucleoside 5′-triphosphates. *Acta Biochim. Biophys. Acad. Sci. Hung. 16*, 131−133.
(63) Milligan, J. F., and Uhlenbeck, O. C. (1989) Synthesis of small RNAs using T7 RNA polymerase. *Methods Enzymol. 180*, 51−62.
(64) Ward, D. C., Reich, E., and Stryer, L. (1969) Fluorescence studies of nucleotides and polynucleotides. *J. Biol. Chem. 244*, 1228−1237.
(65) Rachofsky, E. L., Osman, R., and Ross, J. B. A. (2001) Probing structure and dynamics of DNA with 2-aminopurine: effects of local environment on fluorescence. *Biochemistry 40*, 946−956.
(66) Jean, J. M., and Hall, K. B. (2001) 2-Aminopurine fluorescence quenching and lifetimes: role of base stacking. *Proc. Natl. Acad. Sci. U.S.A. 98*, 37−41.
(67) Seidel, C. A. M., Schulz, A., and Sauer, M. H. M. (1996) Nucleobase-specific quenching of fluorescent dyes. 1. Nucleobase one-electron redox potentials and their correlation with static and dynamic quenching efficiencies. *J. Phys. Chem. 100*, 5541−5553.
(68) Kelley, S. O., and Barton, J. K. (1999) Electron transfer between bases in double helical DNA. *Science 283*, 375−381.
(69) Sandin, P., Borjesson, K., Li, H., Martensson, J., Brown, T., Wilhelmsson, L. M., and Albinsson, B. (2008) Characterization and use of an unprecedentedly bright and structurally non-perturbing fluorescent DNA base analogue. *Nucleic Acids Res. 36*, 157−167.
(70) Dierckx, A., Dinér, P., El-Sagheer, A. H., Joshi, D. K., Brown, T., Grøtli, M., and Wilhelmsson, L. M. (2011) Characterization of photophysical and base-mimicking properties of a novel fluorescent adenine analogue in DNA. *Nucleic Acids Res. 39*, 4513−4524.
(71) Gardarsson, H., Kale, A. S., and Sigurdsson, S. T. (2011) Structure−function relationships of phenoxazine nucleosides for identification of mismatches in duplex DNA by fluorescence spectroscopy. *ChemBioChem 12*, 567−575.
(72) Among the nucleobases, purines (especially guanine) quench the fluorescence of many probes including 2-AP by photoinduced electron transfer process. See ref 67.
(73) Bacterial A-site is one of the oldest and important RNA targets for the discovery of new antibiotics; Gallego, J., and Varani, G. (2001) Targeting RNA with small-molecule drugs: therapeutic promise and chemical challenges. *Acc. Chem. Res. 34*, 836−843.
(74) Hermann, T., and Tor, Y. (2005) RNA as a target for small-molecule therapeutics. *Expert Opin. Ther. Pat. 15*, 49−62.
(75) Ogle, J. M., Carter, A. P., and Ramakrishnan, V. (2003) Insights into the decoding mechanism from recent ribosome structures. *Trends Biochem. Sci. 28*, 259−266.
(76) Moazed, D., and Noller, H. F. (1987) Interaction of antibiotics with functional sites in 16S ribosomal RNA. *Nature 327*, 389−394.
(77) Carter, A. P., Clemons, W. M., Brodersen, D. E., Morgan-Warren, R. J., Wimberly, B. T., and Ramakrishnan, V. (2000) Functional insights from the structure of the 30S ribosomal subunit and its interactions with antibiotics. *Nature 407*, 340−348.
(78) Fourmy, D., Recht, M. I., Blanchard, S. C., and Puglisi, J. D. (1996) Structure of the A-site of *Escherichia coli* 16S ribosomal RNA complexed with an aminoglycoside antibiotic. *Science 274*, 1367−1371.
(79) Vicens, Q., and Westhof, E. (2001) Crystal structure of paromomycin docked into the eubacterial ribosomal decoding A-site. *Structure 9*, 647−658.
(80) Kaul, M., Barbieri, C. M., and Pilch, D. S. (2006) Aminoglycoside-induced reduction in nucleotide mobility at the ribosomal RNA A-Site as a potentially key determinant of antibacterial activity. *J. Am. Chem. Soc. 128*, 1261−1271.
(81) Parsons, J., and Hermann, T. (2007) Conformational flexibility of ribosomal decoding-site RNA monitored by fluorescent pteridine base analogues. *Tetrahedron 63*, 3548−3552.
(82) Xie, Y., Dix, A. V., and Tor, Y. (2009) FRET enabled real time detection of RNA-small molecule binding. *J. Am. Chem. Soc. 131*, 17605−17614.
(83) Kaul, M., Barbieri, C. M., and Pilch, D. S. (2004) Fluorescence-based approach for detecting and characterizing antibiotic-induced conformational changes in ribosomal RNA: comparing aminoglycoside binding to prokaryotic and eukaryotic ribosomal RNA sequences. *J. Am. Chem. Soc. 126*, 3447−3453.

(84) Barbieri, C. M., Kaul, M., and Pilch, D. S. (2007) Use of 2-aminopurine as a fluorescent tool for characterizing antibiotic recognition of the bacterial rRNA A-site. *Tetrahedron* 63, 3567−3574.